Presented at the International Fire & Cabin Safety Research Conference Atlantic City 29 Oct – 1 Nov 2007

A COMPUTATIONAL STUDY OF THE CHARACTERISTICS OF AIRCRAFT POST-CRASH FIRES

Z. Wang, E. R. Galea and F. Jia
FSEG, University of Greenwich, 30 Park Row, Greenwich, London SE10 9LS UK

ABSTRACT

Full-scale furnished cabin fires have been studied experimentally for the purpose of characterising the post-crash cabin fire environment by the US Federal Aviation Administration for many years. In this paper the Computational Fluid Dynamics fire field model SMARTFIRE is used to simulate one of these fires conducted in the C-133 test facility in order to provide further validation of the computational approach and the SMARTFIRE software. The experiment involves exposing the interior cabin materials to an external fuel fire, opening only one exit at the far end of the cabin (the same side as the rupture) for ventilation, and noting the subsequent spread of the external fire to the cabin interior and the onset of flashover at approximately 210 seconds. Through this analysis, the software is shown to be in good agreement with the experimental data, producing reasonable agreement with the fire dynamics prior to flashover and producing a reasonable prediction of the flashover time i.e. 225 seconds. The paper then proceeds to utilize the model to examine the impact on flashover time of the extent of cabin furnishings and cabin ventilation provided by available exits.

1. INTRODUCTION

In aircraft post crash situations, fire is one of the greatest threats to life. The aircraft evacuation certification protocol [1] is designed around the threat of a post crash fire and the resulting onset of non-survivable conditions which may develop within the aircraft passenger cabin. To satisfy aircraft evacuation certification requirements it is necessary to demonstrate – through a full-scale evacuation trial – that it is possible to evacuate all the passengers through half the normally available exits in 90 seconds. The rationale for this time duration is that after 90 seconds, non-survivable conditions are likely to develop within the cabin.

Flashover is a critical point in post crash cabin fire where the fire rapidly grows to engulf the entire cabin [2, 3]. The time to flashover is generally considered to mark the end of the survivability period for those passengers still within the cabin. For many years, the US Federal Aviation Administration (FAA) have undertaken a number of full-scale fire tests involving large external pool fires and furnished cabins to evaluate the nature of the link between burning cabin interior materials and passenger survivability [3, 4, 5]. Through this work, the FAA have developed a test scenario for post-crash fires consisting of an intact fuselage with an opening about the size of a Type A exit ($1.06 \times 1.93 \mathrm{m}^2$) adjacent to an external fuel fire. This test arrangement is considered to create cabin environmental conditions in which survivability is driven by the burning cabin materials and not the external jet fuel fire.

The information gained from full-scale and laboratory-scale fire tests are essential for the

development of improved cabin interiors, assessing passenger survivability and in framing aircraft fire safety regulation. However, realistic full-scale fire tests are time consuming and financially costly. As a result the number of fire scenarios that can be examined are limited. Fire field modelling using Computational Fluid Dynamics (CFD) has been underway for a number of years [6] and some of the earliest applications have involved aircraft cabin fire scenarios [7]. However, early modelling applications [2, 7-10] usually treated the fire as a volumetric source of heat or fuel and simulations were generally intended to represent non-spreading fires. Hence they had limited applicability to regulatory related applications.

In a recent application of fire field modelling [11, 12], Jia et al used the CFD fire simulation software SMARTFIRE [13] to assist the Transportation Safety Board (TSB) of Canada, Fire and Explosion Group, in their investigation of the Swissair MD-11 in-flight fire which resulted in the loss of the aircraft and all passengers and crew. The model developed by Jia et al was capable of modelling flame spread over burnable solid surfaces found in the above ceiling space of the aircraft. The aim of the CFD analysis was to provide insight into the events leading to the accident and to assist investigators in assessing fire dynamics for cause and origin determination.

Besides the convected and radiated heat generated by a fire, toxic gases such as CO, CO_2, HCl, HCN, etc produced by the fire may also pose a serious threat to passengers during a post-crash evacuation. It is thus essential to represent the generation and transport of toxic fire products in aircraft cabin fire simulation. A method, based on the local equivalence ratio concept, has been developed by Wang et al [14, 15] for predicting the generation of toxic combustion products resulting from enclosure fires and implemented within the CFD fire simulation framework of the SMARTFIRE software. This model is capable of predicting toxic gas generation in both well ventilated and vitiated burning conditions. Furthermore, the model has been found to produce reasonable agreement with measured experimental toxic gas concentrations for CO and CO_2 in both the near [14] and far field [15].

The main aim of this study is to further validate the advanced fire models implemented in SMARTFIRE and to investigate how exit availability will impact the onset of flashover and the development of non-survivable conditions within the aircraft cabin. In this paper, the full-scale aircraft fire experiment [5] used to validate the model is described in Section 2, the fire model used in the simulations is described in Section 3 and the simulation results are compared with experimental data and observations in Section 4. The impact of exit availability and hence natural ventilation on the developing cabin atmosphere is analysed in Section 5. Finally, conclusions are drawn in Section 6.

2. THE FAA EXPERIMENT

The fire experiment described in this paper was undertaken by the FAA using their C-133 test article [3-5] in 1989. The schematic of the experimental arrangement is shown in Figure 1. While it is not clear what the exact interior length of the facility is, the facility is 4.52 m wide (at the floor) and has a ceiling height of 2.44 m. The section of the cabin containing the raised floor has a length of 23.37 m. The interior is partitioned into two cabins, a forward cabin and an aft cabin. The cabins are separated by a solid partition (see Figure 1). The forward part of the cabin (containing the raised floor) is 13.7m (45 feet) long while the rear

part of the cabin containing the raised floor is 9.67 m long. The forward cabin was completely furnished and made to represent a typical wide body configuration. There were 14 rows of seats, in a double-triple-double seating configuration, and a single triple seat in front of the galley, resulting in a total of 101 seats. Aircraft seats protected with fire blocking layers were used. The carpet was 90/10 wool/nylon. The side walls and storage bins were assemblies constructed of epoxy-Fiberglas honeycomb panels. The ceiling was composed of flat sheets of epoxy-Fiberglas and epoxy-Kevlar honeycomb panels. In order to enhance the realism of the test, a small number of carry-ons were placed in storage bins and beneath seats.

The cabin rupture (opening) which allows the fire to enter the cabin was represented by the forward Type-A exit, while the rear Type-A exit was used to provide ventilation for the fire (see Figure 1). In this test these were the only two cabin openings providing ventilation for the fire. The fire test was run for a period of 12 minutes.

Temperatures and heat fluxes were measured inside the cabin. Thermocouples were placed 0.025m above the top of the seat back at rows 5, 7, 9 and 15 (an average height of 1.225 m above the floor). The heat flux transducers were located in similar locations to the thermocouples above the seat backs of Rows 1, 4 and 13, pointing towards the ceiling. Concentrations of CO, CO_2 and O_2 were measured at three elevations on the symmetry plane at station 880 (in line with the centre line of the rear exits). The gas sampling location changed from a height of 1.67m to 1.07m and then to 0.45m when the gas analyser became saturated at any one location. Some of the information presented in this paper concerning the experimental facilities and the photographic data were kindly provided by Hill R.G. of the FAA [16].

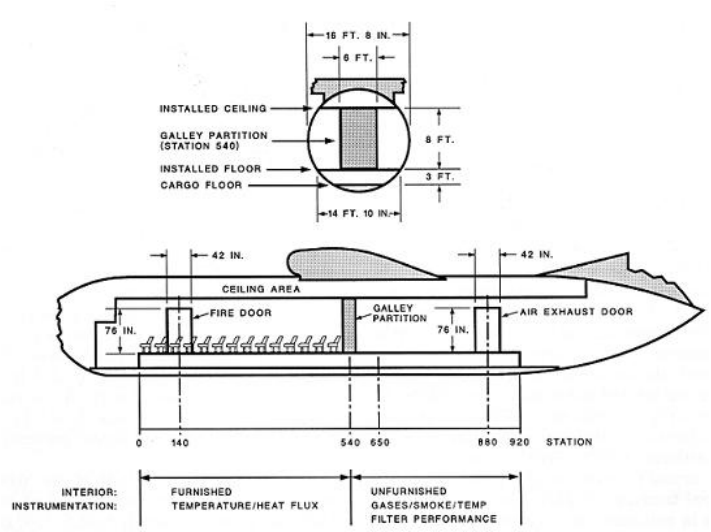

Figure 1: C-133 fully-furnished full-scale test arrangement (reproduced from [3])

3. MATHEMATICAL MODELS AND SIMULATION SET UP

3.1 Fire Models

In fire field modelling, the fluid is governed by a set of three-dimensional partial differential

equations. The generalised governing equation for all variables is expressed in the form of equation (1)

$$\frac{\partial \rho \Phi}{\partial t} + div(\rho \vec{U} \Phi) = div(\Gamma_{\Phi} \nabla \Phi) + S_{\Phi} \quad (1)$$

where Φ represents the fluid vaiable; ρ and $\vec{U}$ are the local density and velocity vector; Γ_{Φ} is the effective exchange coefficient of Φ ; S_{Φ} represents the source term for the corresponding variable Φ and time *t* is an independent vaiable.

A research version of the SMARTFIRE V4.0 [13] software is used as the base model to perform the fire simulations in this study. The SMARTFIRE system has been described in previous publications [11,12,14,15], and so only the relevant new modelling features are addressed here, i.e. the flame spread model and the toxicity model.

Within SMARTFIRE, the ignition of the cabin interior materials is determined by one of the following ignition criteria:

A. The material surface temperature reaches its ignition temperature;
B. The pyrolysis front advances from an adjacent burning cell face to the cell face in question;
C. The flame envelope is in contact with the material and the material surface reaches a critical temperature for a critical period of time;
D. The surface is exposed to a critical heat flux for a critical period of time.

The surface temperature at the cell face is calculated in terms of incident heat flux (the sum of radiative and convective heat flux) and the material properties. The time to ignition of an unburned cell face adjacent to a burning cell face is computed based on the flame spread data. If one of the above ignition conditions is reached, the cell face starts burning. Therefore, once a cell face is ignited, it starts to release a certain amount of fuel according to the burning rate for this material, which is collected from small-scale experiments.

The method developed in [14, 15] for calculating the generation of combustion products is applied in this study to predict toxic gas species concentrations. It is assumed here that there is no combustion if the local equivalence ratio is less than 1.0. With this critical equivalence ratio ϕ_{CR}, a control region is defined as $\phi \geq \phi_{CR}$ and the rest of the computational domain is defined as a transport region. The mass fraction of species i (CO and CO_2), Y_i, is a function of the mixture fraction ξ and the local equivalence ratio ϕ in the control region

$$Y_i = \xi y_i(\phi) \quad (2)$$

where $y_i(\phi)$ is the yield of species *i* when per unit weight fuel is evaporated. The mass fraction of oxygen is expressed with

$$Y_{O2} = 0.233(1-\xi) - \xi y_{O2}(\phi) \quad (3)$$

where 0.233 is the mass fraction of oxygen in the air and $y_{O2}(\phi)$ is the consumption of oxygen when per unit weight fuel is evaporated. In the transport region, the species are calculated by

$$Y_i(\phi) = Y_i(\phi_{CR}) \cdot \xi / \xi_{CR} \quad (4)$$

where ξ_{CR} is the mixture fraction corresponding to the equivalence ratio ϕ_{CR}. Oxygen mass

fraction is

$$Y_{O2}(\phi) = 0.23(1 - \xi / \xi_{CR}) + Y_{O2}(\phi_{CR}) \cdot \xi / \xi_{CR} \quad (5)$$

3.2 Simulation Set Up

Due to time constraints and available computer power it was necessary to make some simplifications to the cabin. While SMARTFIRE is capable of modelling curved surfaces, in this study, the configuration of the cabin has a rectangular cross section (see Figure 2) and the entire cabin is modelled with a constant cabin cross-section. Furthermore, as the actual full size of the cabin interior is not provided its size was estimated from the provided drawings. The length of the aircraft from the end of the raised floor section to the tail is 12.6 m. The length of the cabin section from the end of the raised floor to the back of the cabin is estimated to be some 5.0 m (less than half the distance from the end of the deck to the tail of the aircraft) and the section of cabin to the front of the raised floor is estimated to be 1.5 m. Thus the total length of cabin in the simulation is 29.9 m. The seat base used in the simulations has an area of $0.5 \times 0.5 m^2$ and the seat base is 0.5m above the floor. The top of the seat back is 1.2 m above the floor. These seat dimensions are close to the varied seat dimensions used in fire tests [17].

The outside fuel fire source was located on the left side of the aircraft in the simulation. A rectangular fuel pan with dimensions 2.44m wide and 3.05m long was used in the full-scale post crash cabin fire experiments [5]. The theoretical heat release rate for an open pool fire corresponding to the dimensions used in the experiment is approximately 11.9 MW based on the empirical correlation for large-area Kerosene pool fires [18]. Therefore, a prescribed fire volume with the same dimensions as the fire pan used in the experiment and with a total heat release rate of 10 MW is used in this study. The Eddy Dissipation Model (EDM) model [19] is used for both the external kerosene fire and internal materials fire. The external Kerosene fire is represented using the heat of combustion of Epoxy and the heat release rate of the external fire is artificially increased (to represent the combustion of Kerosene) while ensuring that the a total of 10 MW is released.

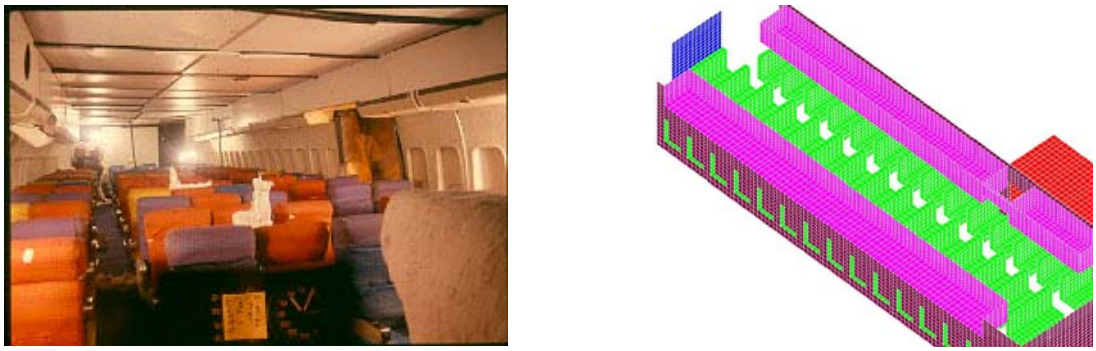

(a) (b)

Figure 2: Forward section of cabin as represented in the experimental set up (figure a) and the SMARTFIRE simulation (figure b).

The computational mesh used in these simulations was non-uniform and consisted of 148,320 cells. This covered both the internal and external regions modelled.

The multi-ray radiation model with 24 rays was used to represent radiative transfer of heat in the simulations.

It proved difficult to obtain accurate material properties for all the materials present in the full-scale fire test [5]. The main interior combustible materials are assumed to have the molecular structure of Epoxy, i.e. $CH_{1.3}O_{0.2}$ [20] however, the properties of Epoxies may vary with their compositions. Approximations to the properties of Epoxy cabin materials used in this study are summarised in Table 1.

Table 1: Properties of Epoxy panel

Density (kg/m^3)	116 [21]	**Conductivity (W/mK)**	0.05 [22]
Downward flame spread rare (m/s)	0.001 [21, 23]	**Downward flame spread rare (m/s)**	0.003 [24]
Heat of combustion (kJ/kg)	12800 [25]	**Specific Heat (J/kgK)**	2090* [13]
CO yield (kg/kg)	0.10 [20]	**CO_2 yield (kg/kg)**	0.87 [20]
HRR (kWmin/m^2/ kW/m^2)	65/65 [24]		

* For fibre board

The species yields in Table 1 are at well ventilated conditions. The yields of combustion products for under-ventilated Epoxy materials fires can be calculated using

$$y(\phi) = y_\infty \left(1 + \frac{\alpha}{e^{(\phi/\beta)^\xi}} \right) \tag{5}$$

where y_∞ are the yields of CO and CO_2 or the consumption of O_2 with well ventilation conditions and ϕ is the equivalence ratio. Other parameters in equation (5) are those for Polystyrene in [20]. With this calculation, the maximal yield of CO for Epoxy panels is 0.30kg/kg. From the experiment, it was noted that the O_2 level was as high as 20% in the rear of the cabin before flashover occurred [5]. This suggests that the combustion was fuel controlled prior to flashover. Therefore, the approximation (5) to the yields of combustion products should be valid at least prior to flashover.

An acceptance criterion for a heat release rule for cabin interior materials was established by the FAA in 1985 [24]. The pass/fail acceptance criteria was set at 65 kW/m^2 for the maximum heat release rate and 65 kW-min/m^2 for two-minute total heat release. Of the materials tested it was noted that '*many were quite close to the 65/65 acceptance criteria, but that very few of them met the criteria with enough margin to risk commitment to production*' [24]. Therefore, it is assumed that the heat release for all of the interior materials in the 'fully-furnished' C-133 fuselage test satisfies the 65/65 requirement. A hypothetical heat release rate curve, which is based on small-scale experimental test data [25], and satisfies the 65/65 standard is depicted in Figure 3.

Within the simulations, a wall emissivity of 0.8 is used for all solid surfaces. The ambient temperature is set to be 15^{O}C. The thickness of the cabin wall is assumed to be 0.05m for the furnished part of the cabin and 0.03m for the unfurnished part. For the furnished part, a moderate conductivity of 0.05 W/mK for insulating materials [22] is taken for the ceilings, side walls and floors of the cabin. The conductivity for the unfurnished parts of the cabin is

assumed to be 0.3W/mK. Because the seats and overhead bins are installed inside the cabin, it is supposed that there is no heat loss through these objects.

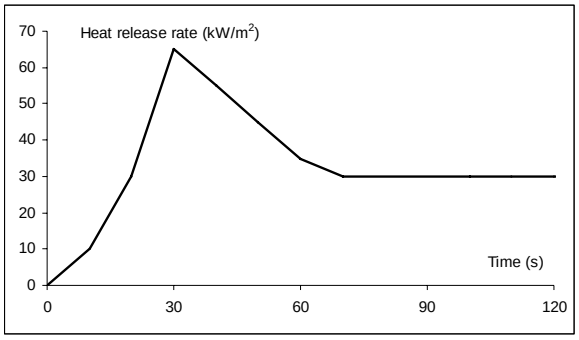

Figure 3 HRR curve for cabin materials

4. SIMULATION RESULTS

4.1 Heat Release rate

The predicted total heat release rate from the burning of interior materials is presented in Figure 4. The predicted heat release rate gradually increased to a local peak value of 335.0 kW at 90 seconds and then slightly decreased and kept to a relatively low value until 140 seconds. From 140 seconds to 200 seconds the heat release rate increased from 343 KW to 509 KW. Between 200 seconds and 270 seconds the heat release rate increases rapidly reaching approximately 5000kW. This rapid rise in heat release rate corresponds to the onset of flashover. Furthermore, the 5000KW heat release rate is consistent with the minimum heat release rate requirement for flashover for the C-133 cabin according to well known correlations such as the Thomas flashover correlation [26]. From Figure 4 the predicted time to the start of the flashover process is estimated to be 225 seconds. From the experiment, flashover is observed to occur at approximately 210 seconds [3, 5].

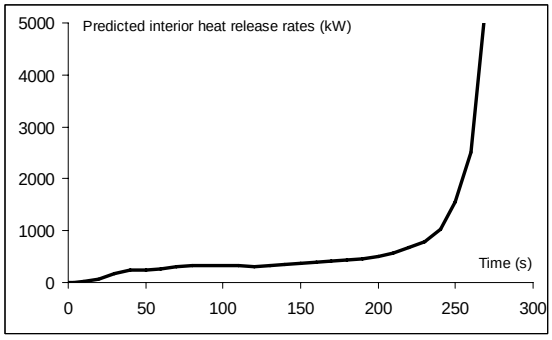

Figure 4: Predicted total heat release rate for cabin interior materials

4.2 Flame Spread

Analyses of several full-scale fire tests using the C-133 facility [3] suggests that the fire

progresses in several distinct phases. First the seat closest to the external fuel fire and rupture (Row 4) are amongst the first material within the cabin to be ignited. The fire then spreads to seat rows ahead and behind of this initial fire location. The ceiling and storage bins above the burning seats are also ignited and start to burn. The fire remained localised and confined to the outboard seats and overhead materials for between 180 seconds and 210 seconds, the latter time being the observed onset of flashover in the experiment. As can be seen in Figure 5, the combustion region in the full-scale experiment was localised in the vicinity of the seats and overhead bins between the 4th and 5th seat rows at 180 seconds after the start of the external fire. The predicted temperatures in the vertical plane passing through the central line of the cabin rupture have reproduced the flame front as observed in the experiment.

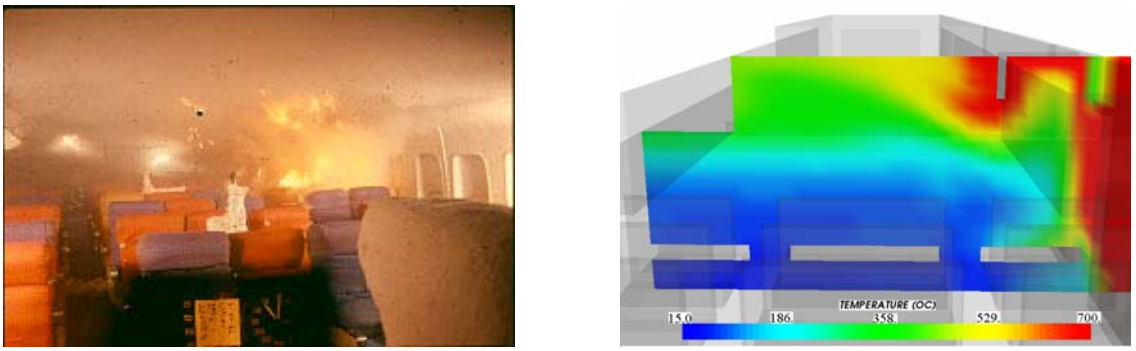

(a) (b)

Figure 5: (a) Observed and (b) predicted flame front in the vicinity of the rupture at 180 seconds

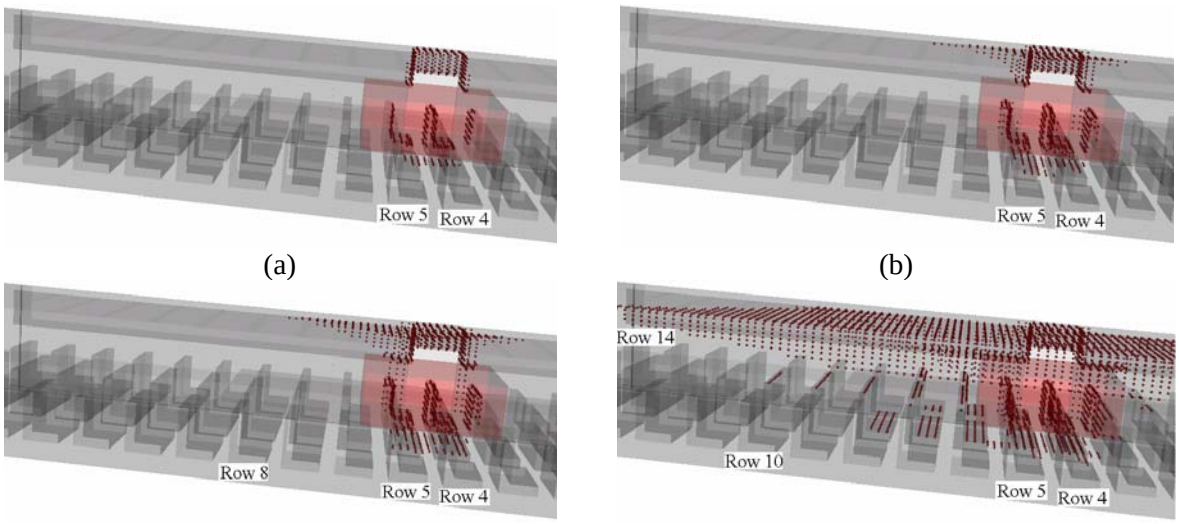

(a) (b)

(c) (d)

Figure 6: Predicted burning locations at (a) 100s; (b) 200s; (c) 220s and (d) 250s

In Figure 6 we present the solid surfaces that are predicted to have ignited. As seen in Figure 6a, the predicted solid surface combustion region at 100 seconds are primarily restricted to the two seats closest to the external fuel fire and the ceilings and the overhead bins in this region. At 200 seconds (see Figure 6b), the predicted burning locations have extended along the overhead bins but remain localised in the identified seating region. This is consistent with

the experimental observations as shown in Figure 5a. At 220 seconds the predicted fire remains localised in the seats but the ceiling and bin combustion front has spread slightly (see Figure 6c). From 220 seconds to 250 seconds, the burning front spreads rapidly, engulfing most of the ceiling bins and spreading to the 10th seat row (see Figure 6d). As can be seen in Figure 6, the predicted flame spread through the overhead bin surfaces is faster than that predicted for the seat rows. These observations are consistent with the estimation that the predicted flashover occurs between 220 and 250 seconds.

4.3 Cabin Atmospheric Conditions and Flashover

Cabin flashover is a critical factor affecting occupant survivability during a post-crash fire dominated by burning cabin materials. The ability to predict the onset of flashover is therefore a key requirement for fire models if they are to have a useful role in regulatory applications associated with cabin fire. The definition of flashover for enclosure fires is generally accepted as occurring when the upper layer gas temperature exceeds 600^{O}C or the heat flux at floor level exceeds 20 kW/m^2 [26]. In the experimental analysis, the onset of flashover was defined as occurring when the temperatures at the top of the seat back in Row 5 begin to rapidly escalate [5]. For consistency, here we use an identical definition to estimate the onset of flashover.

The measured and predicted temperatures at the top of the seat back of the central seat in Row 5 are depicted in Figure 7a. As seen from the measured experimental temperatures, the onset of flashover occurs at approximately 210 seconds [3], after which the measured temperatures escalated rapidly. Before flashover, the measured temperatures were near ambient values. The model predicted temperatures essentially followed these measured trends. However, unlike the extremely sudden change in the measured temperatures at the onset of flashover, the predicted temperatures show a more smooth rise in temperature just before the rapid rise during flashover. From the predicted temperature profile it is estimated that flashover time is approximately 225 seconds.

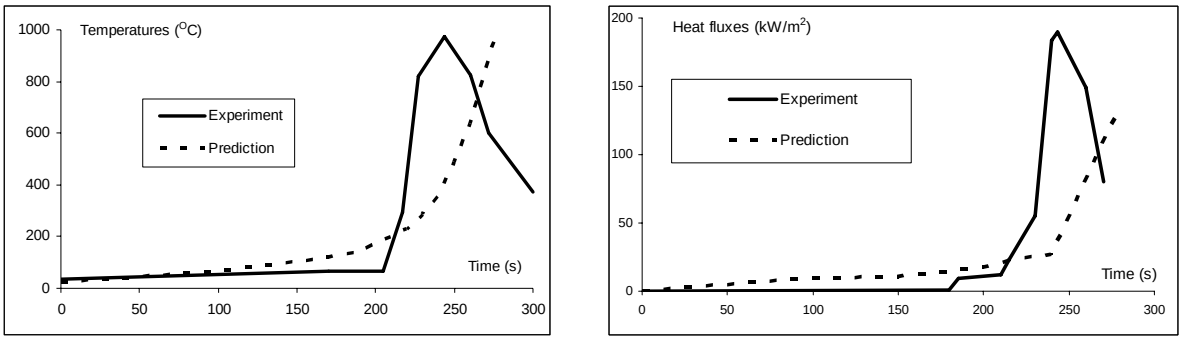

(a) (b)

Figure 7: Measured and predicted (a) temperatures at the seat back top in the 5th row and (b) heat flux at the seat back top in the 4th row

The measured and predicted heat fluxes above the seat back top at Row 4 in the central block are depicted in Figure 7b. As seen in this figure, the measured heat fluxes in the 4th row was very low during the first 180 seconds and reached approximately 9 kw/m^2 before flashover occurred. After flashover, the measured heat fluxes rose rapidly. The measured peak heat flux

was as high as 190kw/m^2 at approximately 240 seconds. The predicted heat fluxes at the same position followed these measured trends. From 50 seconds to 180 seconds, the predicted heat fluxes were approximately 5-13kw/m^2 and increased to approximately 128 kw/m^2 after flashover.

Concentrations of CO and O_2 were measured in the experiment at the symmetry plane at station 880 at heights of 1.67m, 1.06m and 0.45m. The gas sampling location was at 1.67m initially and decreased to a lower position when the gas analyser was saturated. In the experiment, the measured CO concentrations at 1.67m height saturated the gas analyser with a reading of 2.0%, at approximately 250 seconds or 40 seconds after flashover. Therefore, Figure 8 depicts the measured data only at 1.67m while the predicted CO concentrations are provided for both 1.67m and 0.45m. As seen in Figure 8a, the measured CO concentrations were very low within the first 230 seconds, followed by a rapid increase. The predicted trends in CO concentration at a height of 1.67m at station 880 essentially followed the experimental trends. The predicted CO concentrations at a height of 1.67m (high position) gradually varied from 0.001% at 60 seconds to 0.16% at 150 seconds and 0.32% at 260 seconds. After 260 seconds, the predicted CO concentrations rise rapidly. As with the experimental measurements, the rapid rise in CO concentration occurs after the onset of flashover. The predicted CO concentrations at a height of 0.45m were almost zero until 150 seconds. After 150 seconds, there was a gradual increase in CO concentration but the predicted CO concentrations remained less than 0.03% until the predicted flashover time of 225 seconds. The differences between measured and predicted CO concentrations can, in part, be explained by a lack of material data for the cabin materials involved in the fire.

The measured O_2 concentrations at a height of 1.67m on the symmetry plane at station 880 remained at a level higher than 20% until 210 seconds and decreased to approximately 6% at 250 seconds (See Figure 8b). The predicted O_2 concentrations were 19.6% at 210 seconds and remained 19.1% until 250 seconds. While the simulations were only run to 270 seconds, they show the predicted O_2 concentrations beginning to decrease rapidly, following the measured trends. After the predicted flashover, a rapid increase of predicted CO concentrations and a decrease of predicted O_2 concentrations were noted in the simulation (see Figure 8).

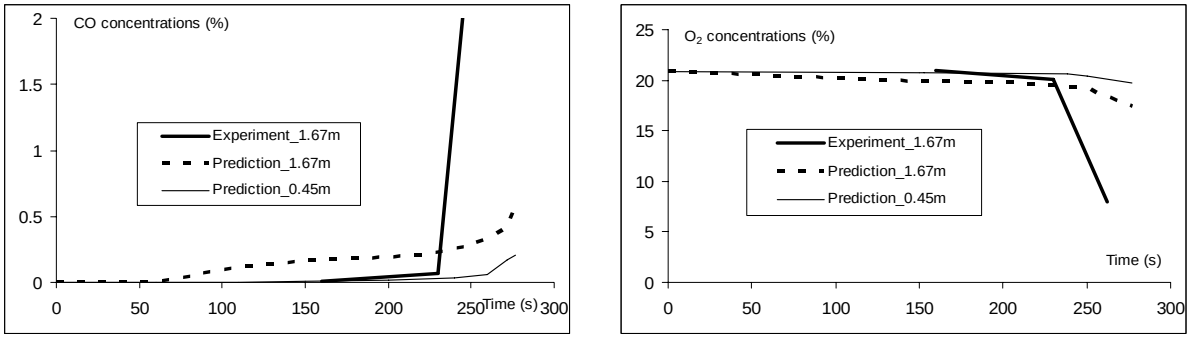

(a) (b)

Figure 8: Measured and predicted concentrations of (a) CO and (b) O_2 at station 880

5. IMPACT OF VENTILATION ON FLASHOVER

In this section we explore the impact of cabin ventilation on the onset of flashover. It is well known that the ventilation conditions and compartment volume can influence flashover behaviour [26]. In an aircraft cabin, the seats and overhead bins occupy a large proportion of the cabin volume and so a partially fitted out cabin is expected to have a different flashover time to a fully fitted out cabin. In the fire experiment examined in this paper [5] and the previous numerical simulation, only half of the cabin was furnished. Here we explore the impact of a fully furnished C-133 fuselage on the time to flashover. In addition, survivable post-crash situations involve passengers attempting to evacuate the aircraft as quickly as possible through as many serviceable exits as possible. It is therefore not unreasonable to assume that many exits are likely to be opened in order to provide an efficient means of escape. Indeed, a recent study into exit availability during post-crash evacuation situations suggests that in approximately 67% of the accidents examined (study involving 42 survivable crashes) at least 50% of the exits were used [27, 28]. With so many exits open, the ventilation of the aircraft cabin is likely to have a significant impact on the developing internal fire. It is therefore important to investigate the impact that additional open exits may have on the time to flashover, and hence the development of non-survivable conditions. In earlier publications Galea and Markatos [2] investigated the impact of exit openings on temperature distribution resulting from non-spreading fire. They found that the more exits that were opened the lower the resulting cabin temperatures and hence the more survivable the conditions. However, in the earlier work the CFD fire models did not include the combustion process or spreading fires. Hence the impact on the fire of the increased cabin ventilation was not considered. With the more sophisticated model used in the current study, these affects can be taken into consideration.

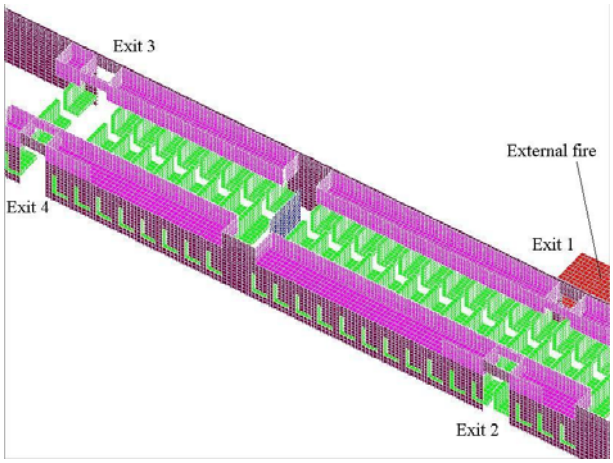

Figure 9: Representation of the fully furnished C-133 cabin with SMARTFIRE (ceilings are removed to allow visualisation of the inside cabin)

To examine these conditions a series of hypothetical fire situations similar to the test fire conducted by the FAA, but in which the cabin is fully furnished and the number of open exits varies, are simulated using the SMARTFIRE fire simulation software. The aircraft geometry is identical to that used in the previous simulation, but in these scenarios the C-133 cabin is

fully furnished. The entire cabin therefore contains 168 seats (see Figure 9) compared to the 101 seats in the previous simulations.

In all cases the external fuel fire is located by the open exit 1 but various other exits may be open during the simulations. It should be noted in all of the cases examined there is not external wind. The outside conditions are assumed to be calm apart from the wind conditions generated by the external fire. The full scenario description is presented in Table 2. The scenario involving furnishings in only the forward cabin is termed the 'Base Case'.

Table 2: Scenario description

Scenario	Furnishing arrangement	Open Exits
Base Case	Forward cabin only	1 and 3
1	Forward and aft cabin	1 and 3
2	Forward and aft cabin	1, 3 and 4
3	Forward and aft cabin	1, 2 and 4
4	Forward and aft cabin	1, 2, 3 and 4

The results for these scenarios are summarised in Table 3. The times to flashover are calculated in terms of the seat top temperatures at Row 5. As seen in Table 3, flashover occurs in the Base Case and Scenario 1 and 2. Flashover is not observed in Scenarios 3 and 4 over the 480 seconds of the simulation. With the cabin fully furnished and with the same ventilation conditions as in the Base Case, we note that flashover occurs at 187 seconds (Scenario 1), some 38 seconds or 17% sooner. This suggests that it is essential to have the cabin fully fitted if reliable flashover times are to be produced. The predicted time to flashover in Scenario 1 is 100% longer than the evacuation performance requirement of 90 seconds. Clearly, the time to flashover will be dependent on the size of the cabin, and thus smaller aircraft are likely to have shorter flashover times.

Table 3: Predicted flashover times for the various exit scenarios

	Base case	Scenario 1	Scenario 2	Scenario 3	Scenario 4
Open Exits	Exits 1 and 3	Exits 1 and 3	Exits 1, 3, 4	Exits 1, 2, 4	Exits 1-4
Furnishing	Forward half	Full	Full	Full	Full
Time to Flashover (s)	225	187	193	--	--

If the two furthest exits from the fire are open (Scenario 2) the flashover time increases by 6 seconds to 193 seconds. This represents only a modest 3.2% increase in the flashover time. However, in Scenarios 3 and 4 the exit opposite the external fire is opened. In these cases, even with only two additional exits open (i.e. Scenario 3) flashover is not observed within the first 480 seconds. This is because a large proportion of the hot fire gases and thermal radiation generated by the internal fire are vented directly to the outside of the cabin via the opening. This case may be considered exceptional in that the forward number 2 exit was exactly opposite the external fire and hence the developing internal fire. It is not clear if such a profound impact on the time to flashover would be produced if the exit was not in line with the developing internal fire.

A detailed analysis of the impact the fire atmosphere resulting from the various ventilation scenarios has on evacuation is examined in [29], which is also presented at this conference.

6. CONCLUSION

The CFD fire simulation software SMARTFIRE was used to simulate a full-scale fire test conducted by the FAA in their C-133 test facility. The fire simulation model incorporated a range of sophisticated sub-models including; flame spread model, the EDM combustion model, a multi-ray radiation model and a toxicity generation model based on the local equivalence ratio. Model parameters involved in the simulations were derived from the fire experiment where possible or from published data.

Based on predicted temperatures at a given location, the SMARTFIRE software predicted that the cabin would flashover in some 225 seconds while the observed flashover, based on the same criteria, was observed to flashover in 210 seconds. The predicted flashover time is considered to be a reasonable approximation to the measured flashover times given the uncertainties within some of the model parameters. The simulation also produces reasonable predictions of the moving burning front when compared with experimental observation. In particular, the model correctly predicted that the fire would remain localised and confined to the outboard seats and overhead materials prior to flashover. While the predicted CO concentrations were low, being between 0.001% and 0.16% from 60 to 150 seconds, they were higher than the measured values. However, the predicted CO and O_2 concentrations did follow observed experimental trends. This simulation suggests that the SMARTFIRE software is capable of reproducing, to a reasonable level of accuracy, the complex fire dynamics associated with flashover fires in aircraft cabins.

The SMARTFIRE software was then used to examine the impact of varied exit openings and the extent of the cabin furnishings on the time to flashover. The simulations demonstrate that the nature of the furnished state throughout the cabin will affect the time to flashover. This is considered an important observation for full-scale fire testing as it suggests that it is not sufficient to simply furnish the portion of the cabin that will be involved in the fire. However, the most important observation was that the flashover time was significantly affected by the nature of the cabin ventilation provided by open cabin exits. It was shown that opening cabin exits tends to delay the time to flashover and if the exit opposite the internal fire is open, providing a direct route for hot gases to vent to the exterior, flashover did not occur within the first 480 seconds of the fire. Both sets of observations have implications for the industry imposed 90 second egress time requirement.

Investigation is continuing with an analysis of the sensitivity of the predicted results to material properties and to include the generation of HCl produced by the combustion of cabin materials.

ACKNOWLEDGMENT

Professor Galea is indebted to the UK CAA for their financial support of his personal chair in Mathematical Modelling at the University of Greenwich.

REFERENCES

[1] Title 14, Code of Federal Regulations (14 CFR), Federal Aviation Regulations, Washington, USA, 1999.
[2] Galea E. R. and Markatos N. C., Forced and natural venting of aircraft cabin fires, AGARD Conference Proceedings, No. 467, Aircraft Fire Safety, Sintra, Portugal, May 22-26, 1989.
[3] Sarkos C. P., Application of full-scale fire tests to characterize and improve the aircraft postcrash fire environment, Toxicity, Vol. 115, pp. 79-87, 1996.
[4] Sarkos C. P., Hill R. G. and Howell W. D., The development and application of a full-scale wide-body test article to study the behaviour of interior materials during a post crash fuel fire, Journal of Fire and Flammability, Vol. 13, 1982, pp. 172-202.
[5] Sarkos C. P. and Hill R. G., Characteristics of aircraft fires measured in full-scale tests, Advisor Group for Aerospace Research and Development (AGARD; Neuilly-Sur-Siene, France) Conference Proceedings, No. 467 on Aircraft Fire Safety, May 22-26, 1989, Sintra, Portugal.
[6] Galea, E.R., On the field modelling approach to the simulation of enclosure fires, J. Fire Protection Engng 1,11-22, 1989.
[7] Galea E. R. and Markatos N. C., A Review of Mathematical Modelling of Aircraft Cabin Fires. App Math Mod, Vol 11, 161, 1987.
[8] Hadjisophocleous G. V., Sousa A. C. M. and Venart J. E. S., Time development of convection flow patterns in aircraft cabins under post-crash fire exposure, AGARD Conference Proceedings, No. 467, Aircraft Fire Safety, Sintra, Purtugal, May 22-26, 1989.
[9] Galea E. R. and Hoffmann N., Using mathematical models to predict the development of aircraft cabin fires, Advisor Group for Aerospace Research and Development (AGARD; Neuilly-Sur-Siene, France) Conference Proceedings, No. 587 on Aircraft Fire Safety, May 14-17, October 1996, Dresden, Germany.
[10] Suo-Anttila J., Gill W., Gallegos C. and Nelsen J., Computational fluid dynamics code for smoke transport during an aircraft cargo compartment fire: transport sovlver, graphical user interface, and preliminary baseline validation, DOT/FAA/AR-03/49, 2003.
[11] Jia, F., Patel, M. K., Galea, E. R., Grandison, A. and Ewer, J., CFD fire simulation of the Swissair flight 111 in-flight fire Part I: Prediction of the pre-fire air flow within the cockpit and surrounding areas, The Aeronautical Journal of the Royal Aeronautical Society, pp.44, January 2006.
[12] Jia F., Patel M.K., Galea E.R., Grandison A. and Ewer J., CFD Fire Simulation of the Swissair Flight 111 In-flight Fire – Part II: Fire Spread within the Simulated Area, The Aeronautical Journal of the Royal Aeronautical Society, pp. 303, May 2006.
[13] Ewer, J., Grandison, A., Jia, F, Galea, E., Knight, B. and Patel, M., User guide and technical manual, SMARTFIRE V4.0, Fire Safety Engineering Group, University of Greenwich, UK, 2004.
[14] Wang Z., Jia F., and Galea E.R., Predicting toxic gas concentrations resulting from enclosure fires using local equivalence ratio concept linked to fire field models, Fire and Materials, Vol. 31, No. 1, 2007, pp 27-51.
[15] Wang Z., Predicting toxic gas concentrations resulting from enclosure fires using the local equivalence ratio concept linked to fire field models, PhD Thesis, The University of Greenwich, 2007.
[16] Hill, R.G., Private communication, FAA, U.S., 2006

[17] Hill R.G., Brown L.J., Speitel L., Johnson G.R. and sarkos C., Aircraft seat fire blocking layers: effectiveness and benefits under various scenarios, DOT/FAA/CT-83/43, 1984.
[18] Babrauskas V., Simple case of heat release rates (b) Pools, in Heat release in fires, Edited by Babrauskas V. and Grayson S. J., 1996.
[19] Magnussen B.F. and Hjertager B.H., "On mathematical modelling of turbulent combustion with special embassies on soot formation and combustion", 16th Symp. (Int.) on Combustion, the Combustion Institute, 1977.
[20] Tewarson, A., generation of heat and chemical compounds in fires, in 'the SFPE handbook of fire protection engineering', 2nd edition, published by the National fire protection, 3.53-3.124, 1995.
[21] Lyon R. E., Castelli L. M. and Walters R., A fire resistant epoxy, DOT/FAA/AR-01/53.
[22] Appendix B, in 'the SFPE handbook of fire protection engineering', 2nd edition, published by the National fire protection, A.26-A.36, 1995.
[23] Quintiere J.G., Surface flame spread, SFPE Handbook of Fire Protection Engineering, 2nd edition, published by the National fire protection, 1995, pp2-205.
[24] Peterson J. M., FAA regulations on aircraft cabin wall materials, in Heat release in fires, Edited by Babrauskas V. and Grayson S. J., 1996.
[25] Parker W. J. and Filipczak R., Modelling the heat release rate of aircraft cabin panels, DOT/FAA/CT-92/3, 1993.
[26] Peacock D., Reneke P. A., Bukoski R.W. and Babrauskas V., Definition flashover for fire hazard calculation, Fire Safety Journal, Vol. 32, 1999, pp. 331.345.
[27] Galea, E.R., Finney, K., Dixon, A.J.P., Siddiqui, A and Cooney, D., Aircraft Accident Statistics and Knowledge Database: Analyzing Passenger Behaviour in Aviation Accidents. AIAA Journal of Aircraft, Vol 43, Number 5, pp 1272-1281, 2006.
[28] Galea, E.R., Togher, M., Lawrence, P., "Investigating the Impact of Exit Availability on Egress Time using Computer based evacuation simulation." Proceedings of the International Aircraft Fire & Cabin Safety Conf, Oct 29 – Nov 1, 2007, Atlantic City USA. http://www.fire.tc.faa.gov/2007Conference/conference.asp.
[29] Wang, Z., Togher, M., Galea, E.R., Jia, F., and Lawrence, P., "Predicting the likely impact of aircraft post-crash fire on aircraft evacuation using fire and evacuation simulation." Proceedings of the International Aircraft Fire & Cabin Safety Conf, Oct 29 – Nov 1, 2007, Atlantic City USA. http://www.fire.tc.faa.gov/2007Conference/conference.asp.